

| Library Name | Sample | Barcode Sequence |
|---------------------|---------------|-------------------------|
| Atlas_10wk | E2 | GGTCGAGAGCATTCA |
| Atlas_10wk | E3 | CTTGCCGCATGTCAT |
| Atlas_10wk | E4 | AAAGCATTCTTCACG |
| Atlas_20wk | E2 | GGTCGAGAGCATTCA |
| Atlas_20wk | E3 | CTTGCCGCATGTCAT |
| Atlas_20wk | E4 | AAAGCATTCTTCACG |
| Aducanumab | E2_isocon | GGTCGAGAGCATTCA |
| Aducanumab | E3_isocon | CTTGCCGCATGTCAT |
| Aducanumab | E4_isocon | AAAGCATTCTTCACG |
| Aducanumab | E2_aducanumab | CTTTGTCTTTGTGAG |
| Aducanumab | E3_aducanumab | TATGCTGCCACGGTA |
| Aducanumab | E4_aducanumab | TATAGAACGCCAGGC |
| A β uptake | E2_lo | GGTCGAGAGCATTCA |
| A β uptake | E3_lo | CTTGCCGCATGTCAT |
| A β uptake | E4_lo | AAAGCATTCTTCACG |
| A β uptake | E2_hi | CTTTGTCTTTGTGAG |
| A β uptake | E3_hi | TATGCTGCCACGGTA |
| A β uptake | E4_hi | TATAGAACGCCAGGC |

Supplemental Table 1, Related to STAR Methods: Barcode sequences for demultiplexing of single cell libraries. Samples from the indicated library were stained with TotalSeq-C hashing antibodies with the corresponding barcode sequence in the table. These sequences can be used to demultiplex raw reads with Cell Ranger multi, using read R2 and pattern 5PNNNNNNNNNN(BC).

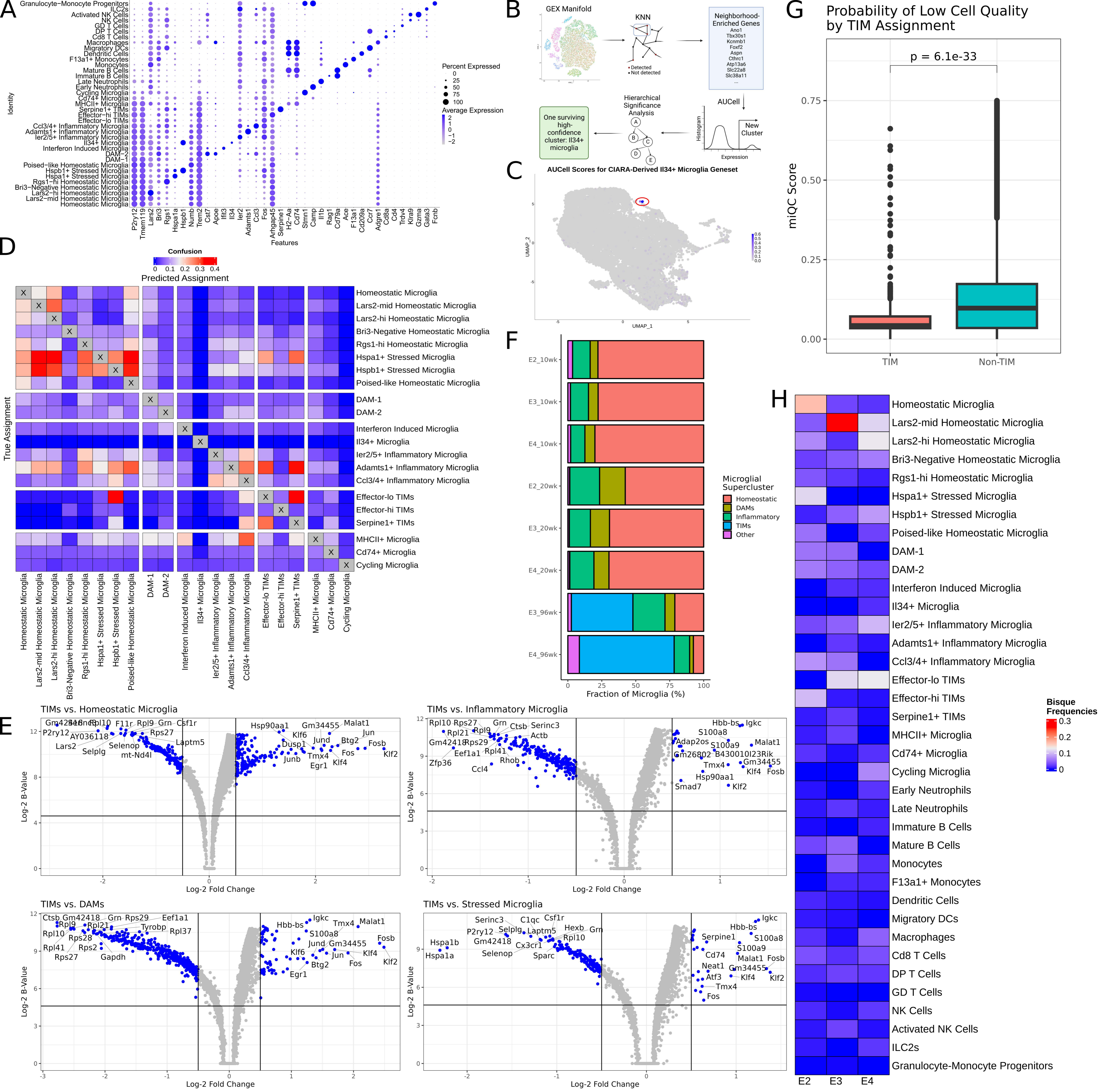
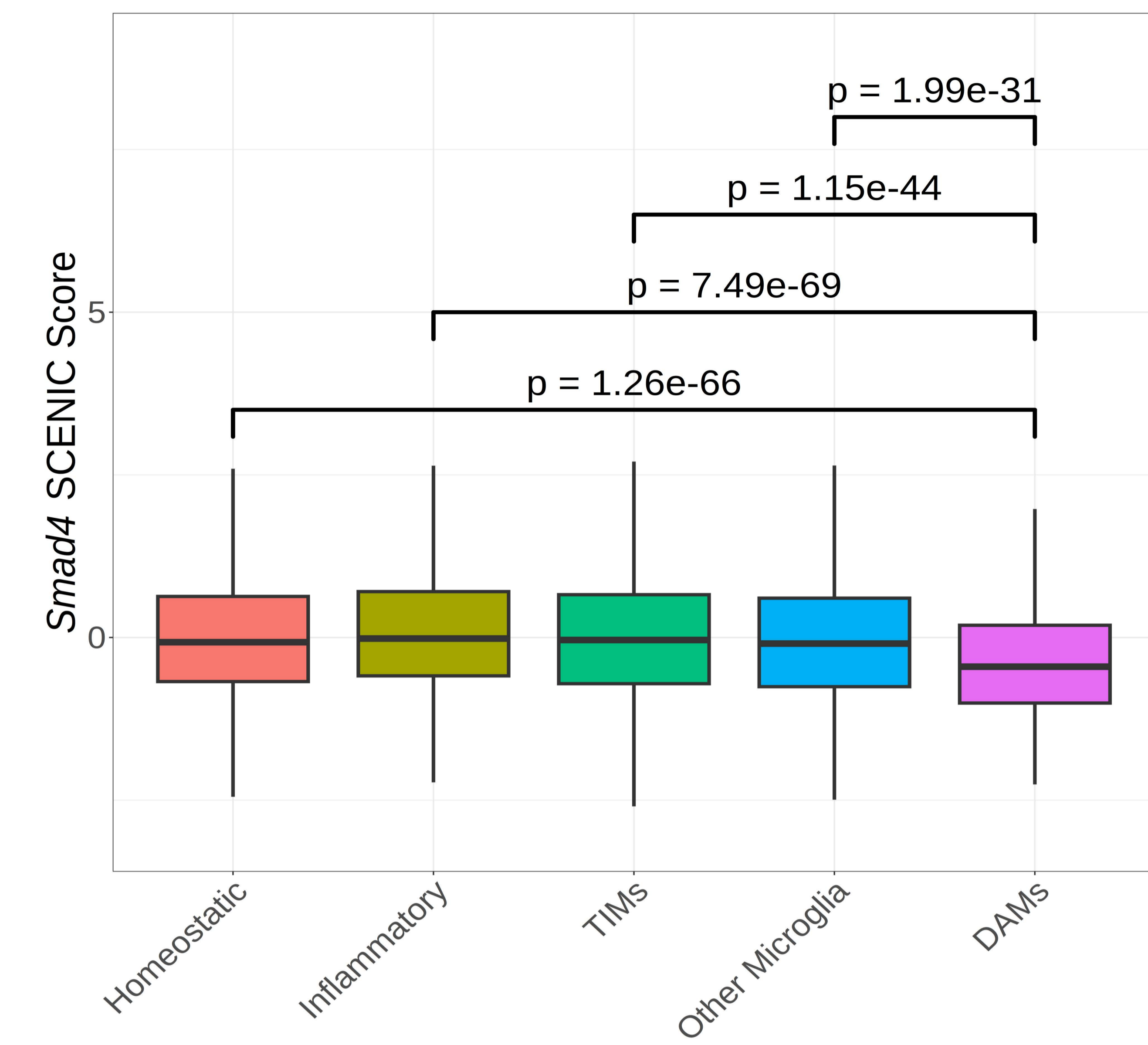
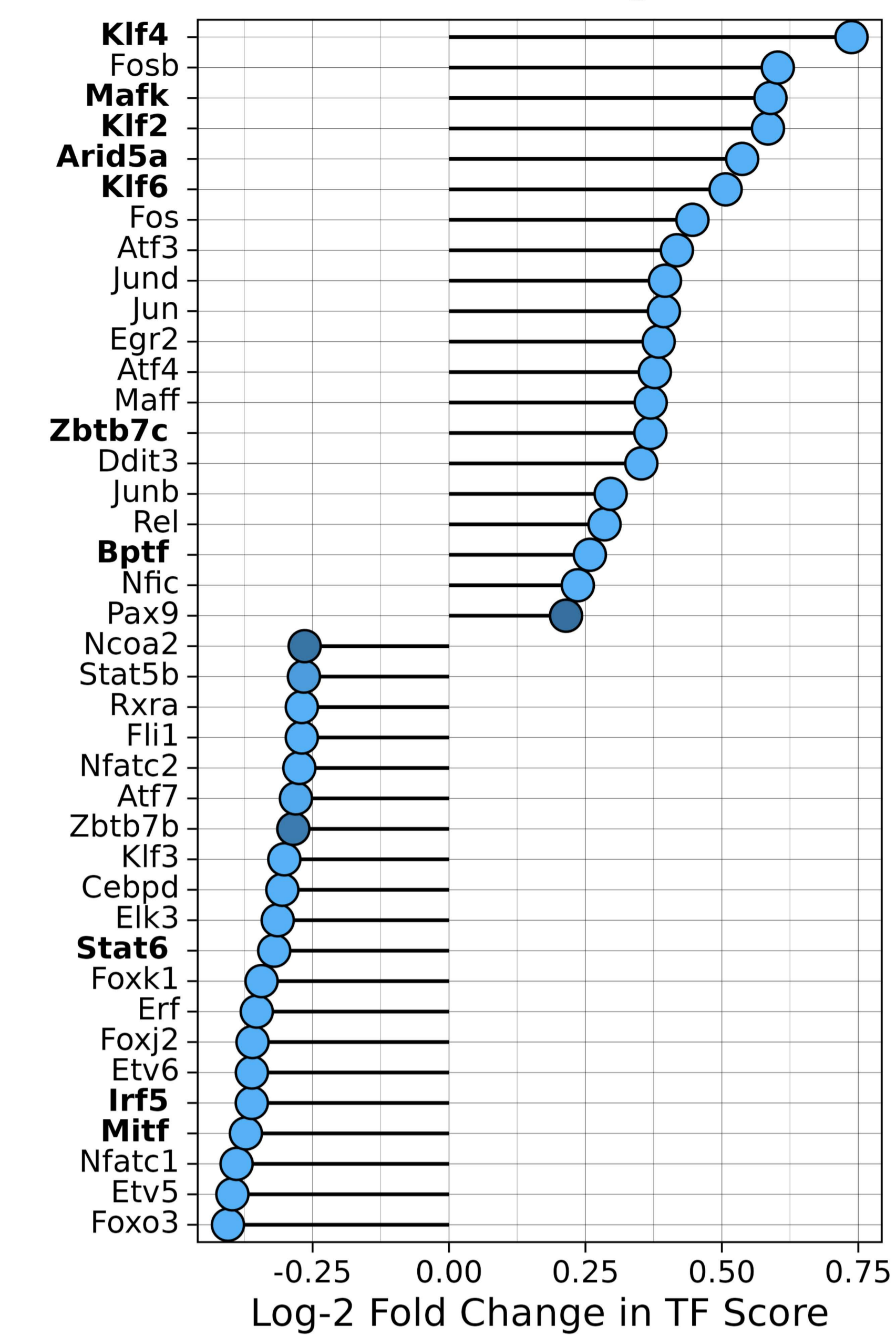


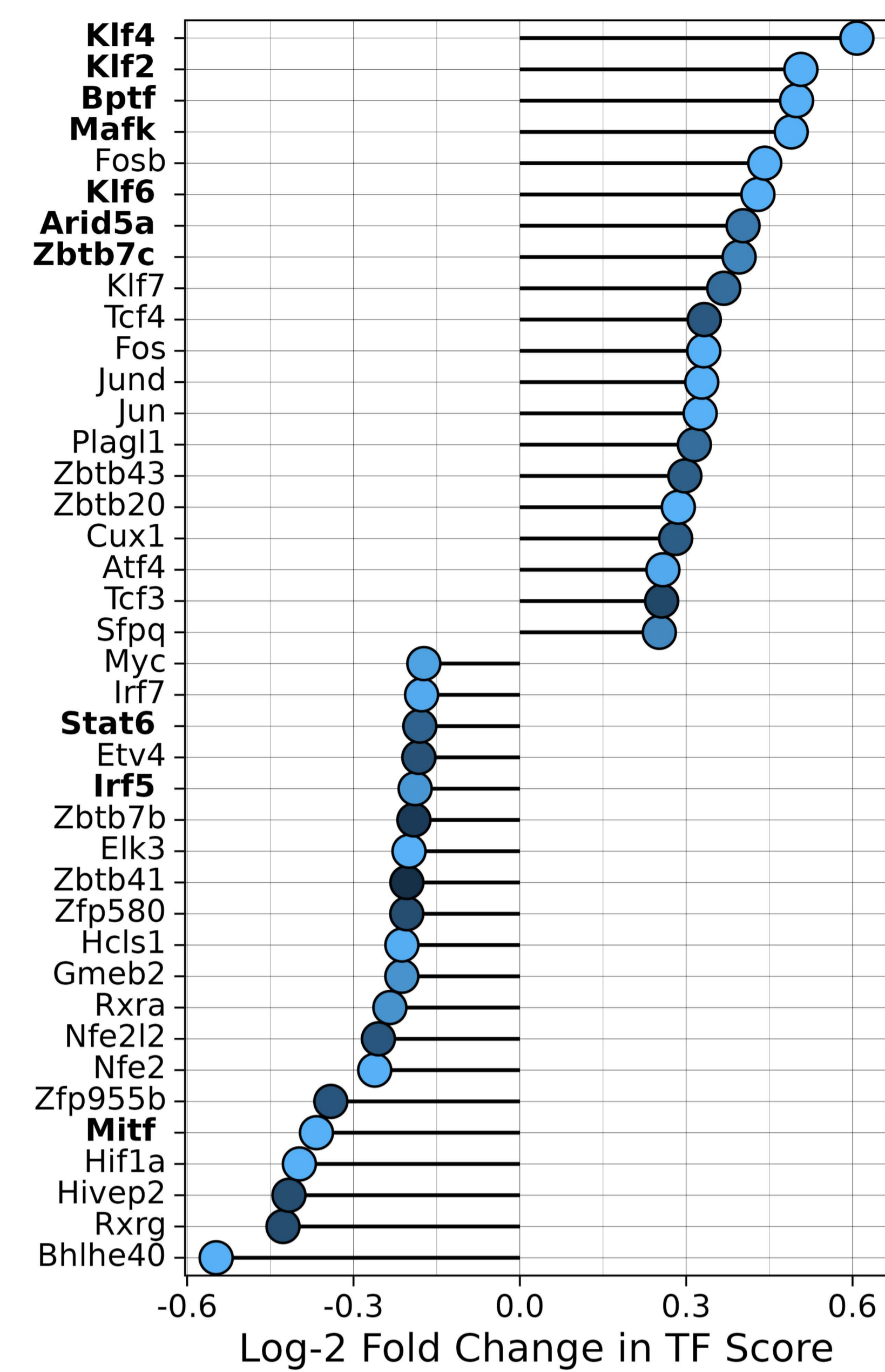
Figure S1, Related to Figure 1: Clustering of the integrated atlas. (A) Dotplot of markers used in supervised annotation of clusters. (B) Schematic of the CIARA pipeline for identification of rare cell types. (C) Feature plot of scores generated by CIARA, a KNN-based scheme for identification of rare cell types, for the top 14 genes associated with the signature of I134⁺ microglia, in UMAP space. Note the consistent signal in a region to the top right of the UMAP; after AUCell, 11 cells passed thresholding and were annotated as a microcluster of I134⁺ microglia. (D) The resulting confusion matrix from training a 100-tree pairwise random forest classifier on raw count data from cells of each cluster for 25 iterations. (E) Volcano plots of differentially expressed genes between TIMs and the indicated microglial superclusters. Superclusters are defined as in Figure 1C. The B-statistic is the log-odds that a gene is differentially expressed. Statistics were calculated using voom normalization and empirical Bayesian estimation through the limma package. (F) Stacked barplot of the fraction of microglia in each sample in the atlas coming from each microglial supercluster. (G) miQC scores for all TIM and non-TIM cells in the atlas. Higher score indicates a higher probability that the cell is low quality or compromised. p-values calculated by Wilcoxon test. (H) Heatmap of decomposition estimates for all clusters made by Bisque.

A**B**

TIMs vs. Homeostatic Microglia



TIMs vs. DAMs



TIMs vs. Inflammatory Microglia

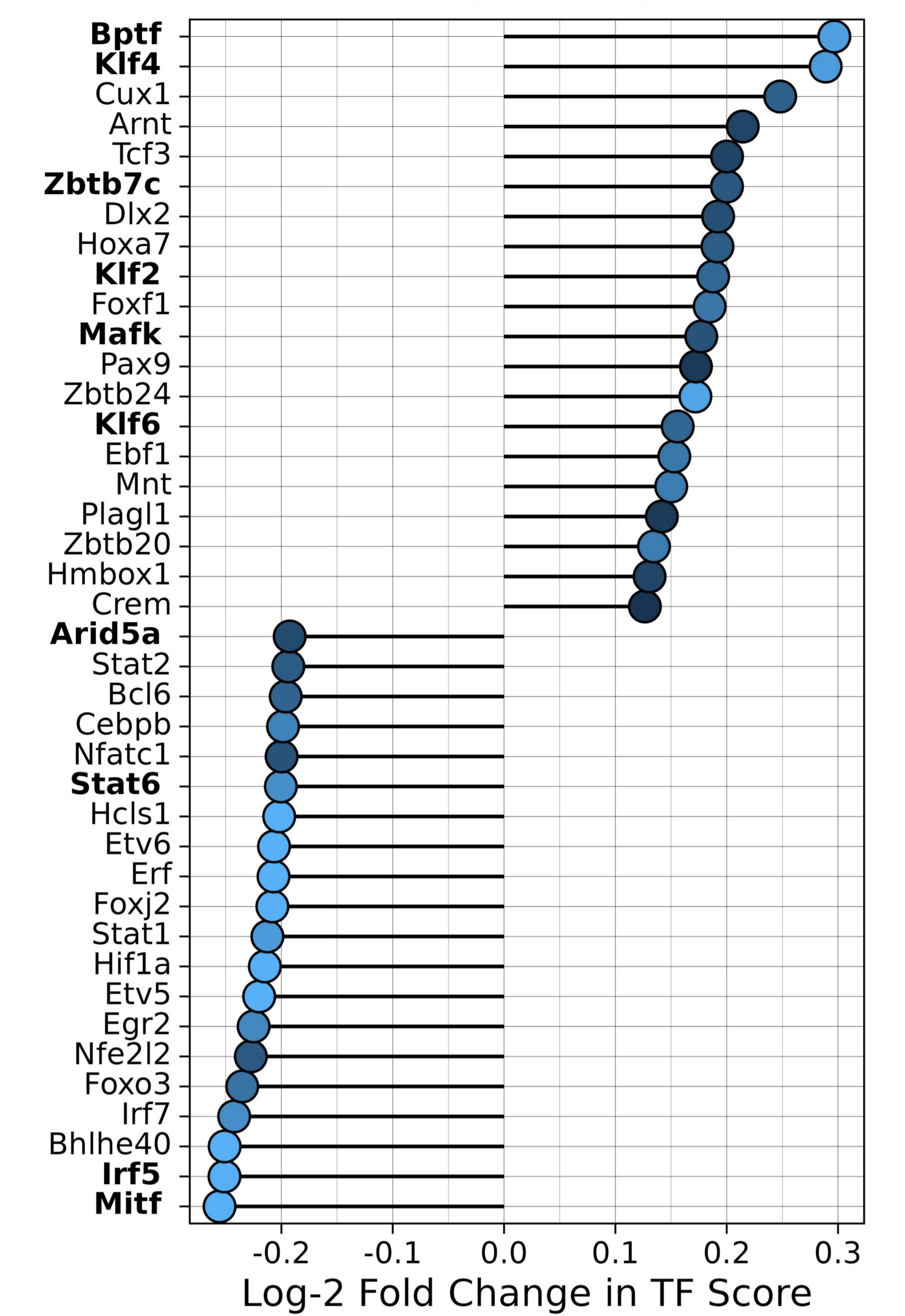
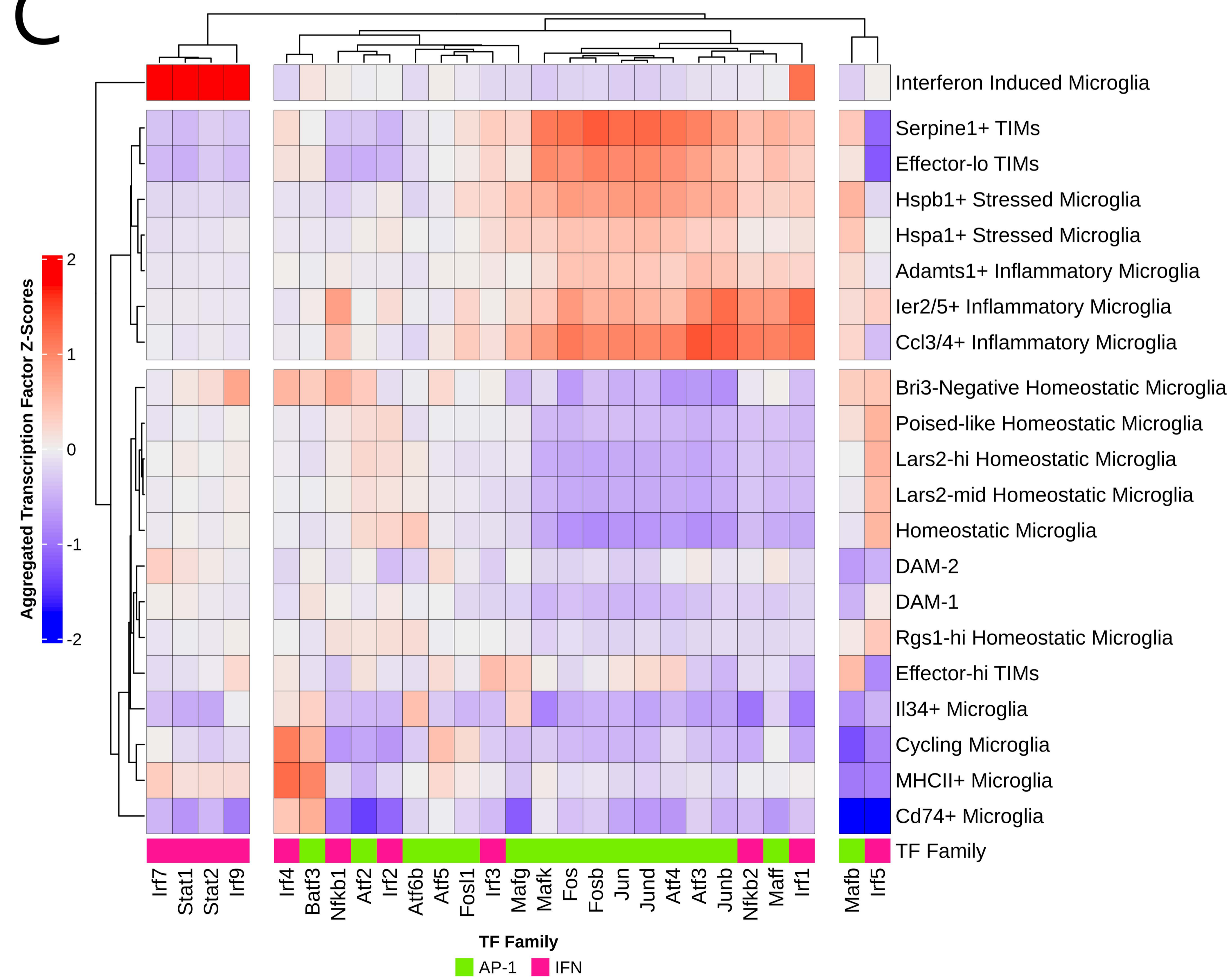
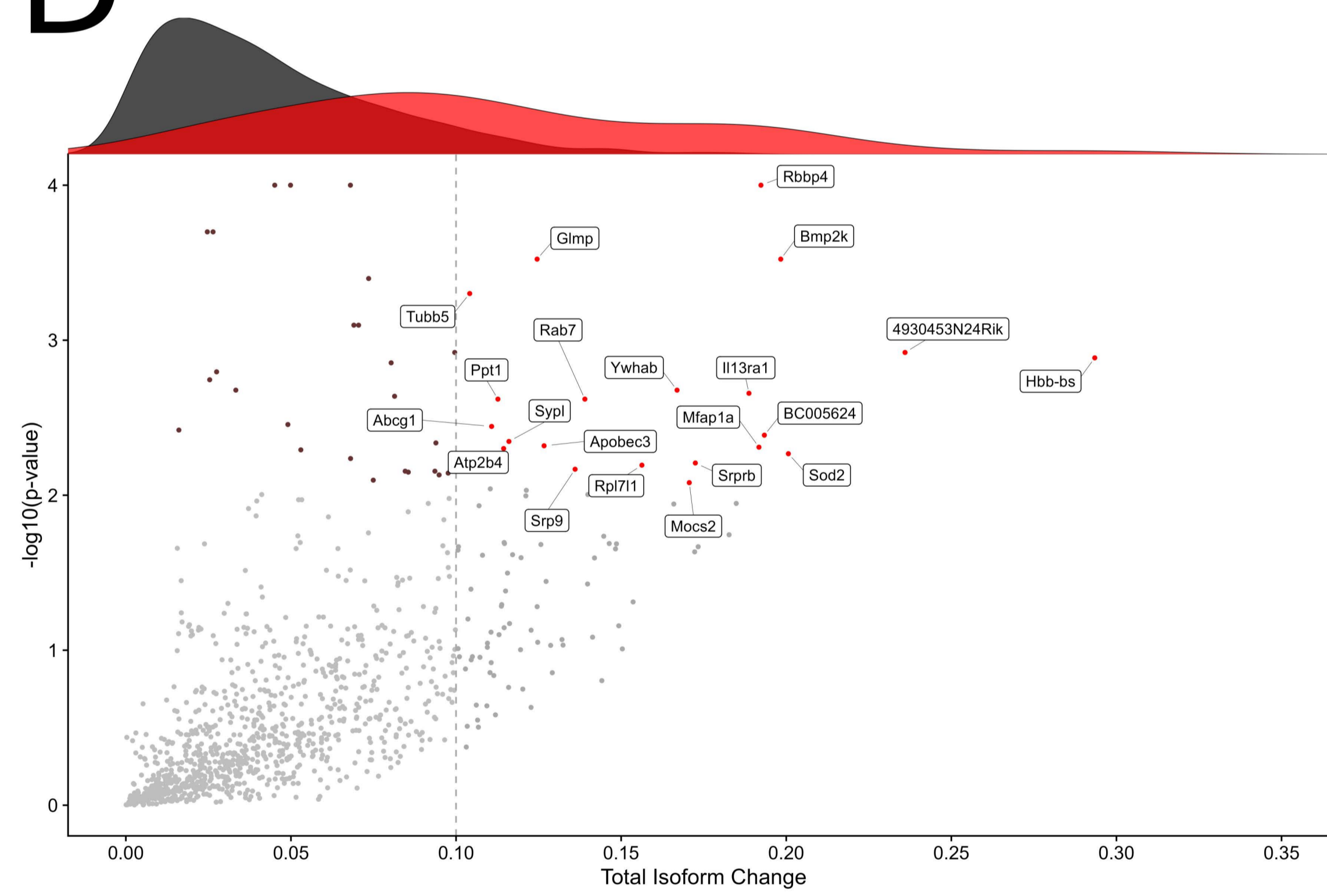
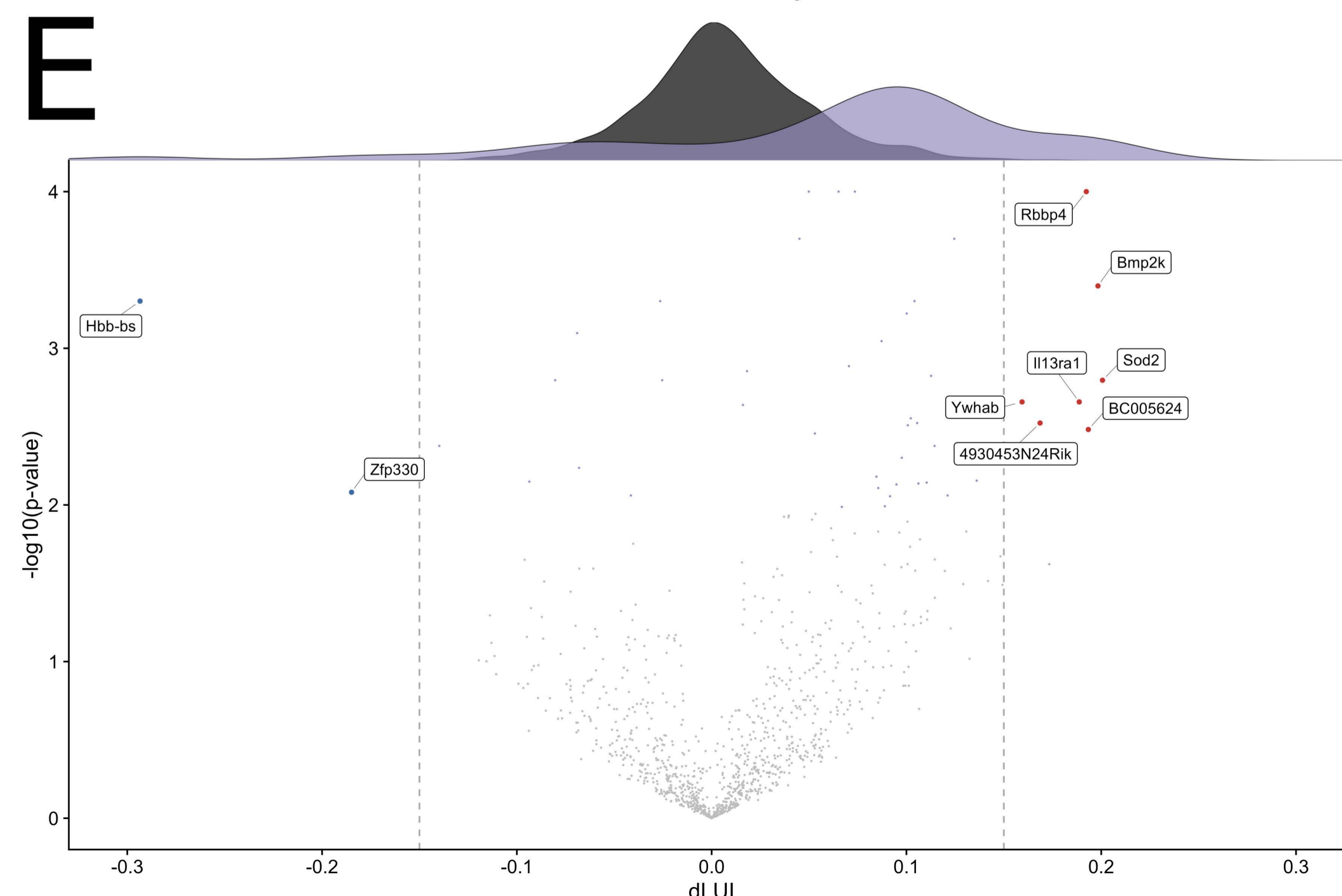
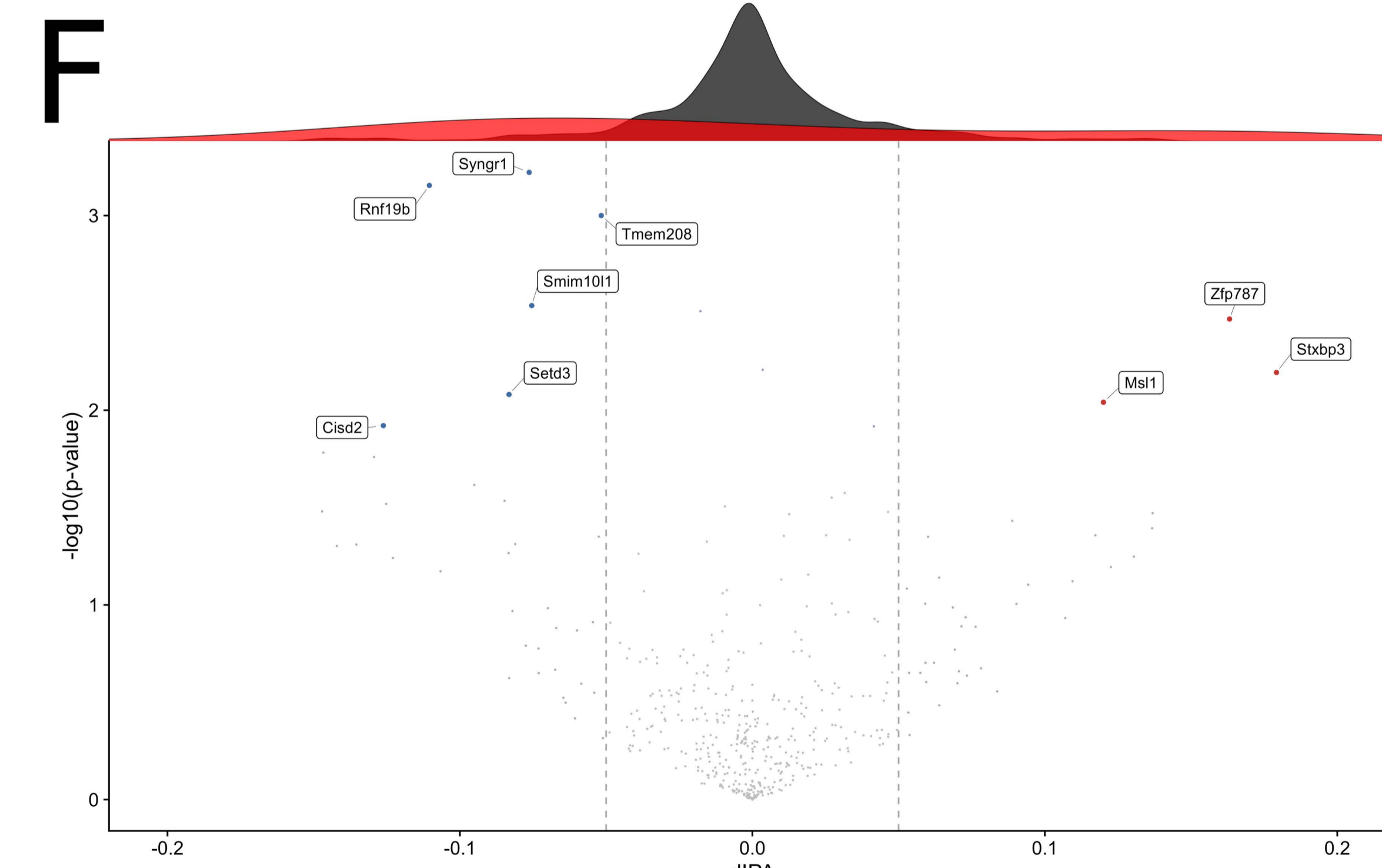
**C****D****E****F**

Figure S2, Related to Figure 2: Further analysis of microglia from 96-week-old *APOE3* and *APOE4* mice. (A) Boxplots of *Smad4* regulon scores generated by SCENIC. p-values calculated by Wilcoxon test with Holm-Bonferroni adjustment. Superclusters are mirrored from Figure 2E. (B) Lollipop plots of differentially enriched SCENIC-derived regulons between TIMs and each indicated microglial supercluster. Superclusters are defined as indicated in Figure 1C. Positive values indicate increased strength in TIMs. Bolded transcription factors are shared across all three comparisons. (C) Heatmap of SCENIC scores for all AP-1 factors and interferon-related factors. (D) Plot of the Wasserstein distance in isoform usage of the indicated genes between *APOE3* and *APOE4* mice. Significance calculated via bootstrap resampling. (E) Same as (D) but plotting differential long isoform usage (long 3'UTR index, or LUI). Positive values indicate increased long isoform usage in *APOE4*. (F) Same as (D) but plotting differential intronic polyadenylation. Positive values indicate increased long isoform usage in *APOE4*.

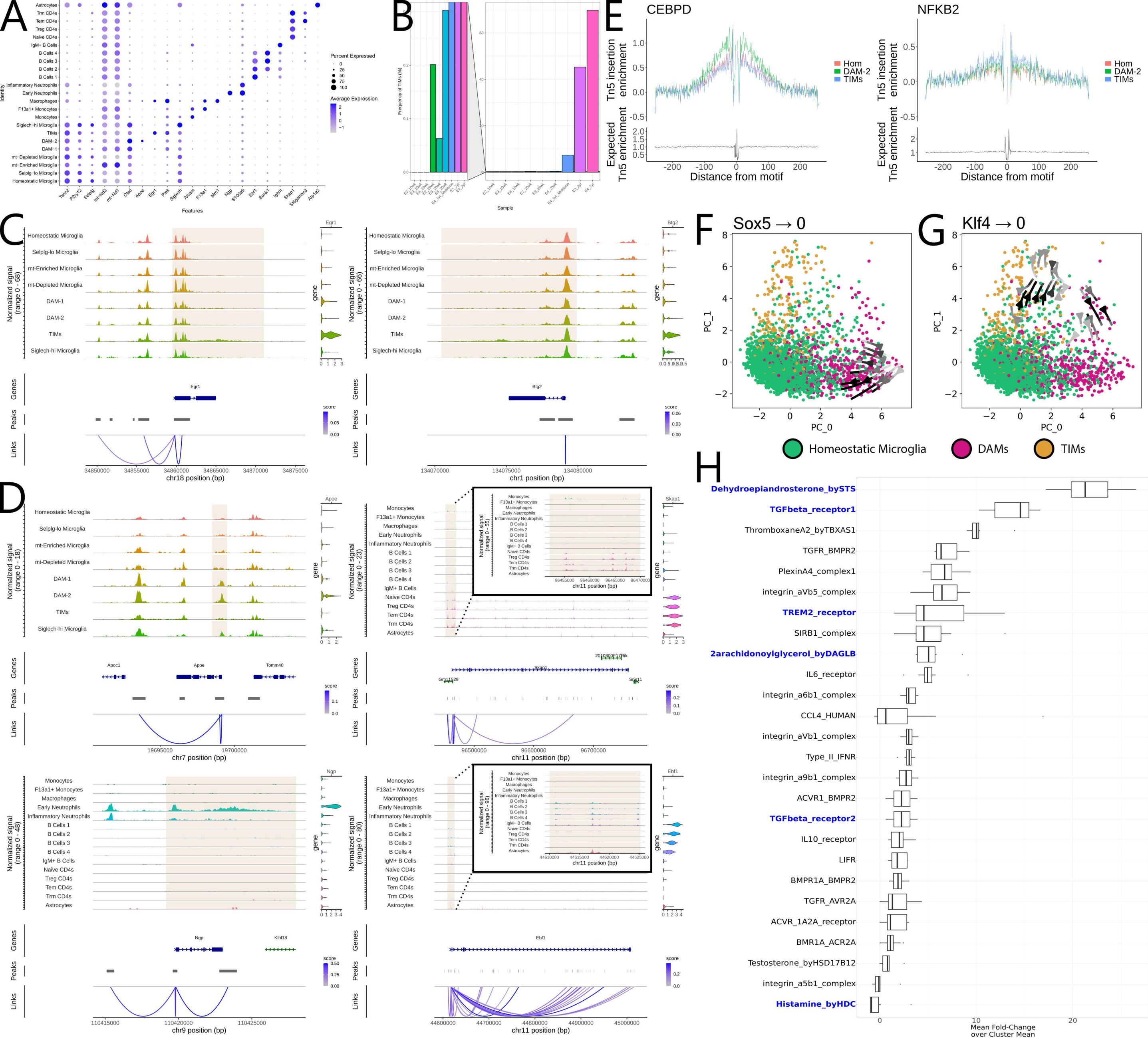


Figure S3, Related to Figure 3: Further analysis of the multiome dataset. (A) Dotplot of markers used in supervised annotation of clusters. (B) Barplot of the frequency of TIMs from each sample across the integrated atlas and the multiome dataset. (C) Coverage plot showing concordance between RNA and ATAC modalities for *Egr1* and *Btg2*, two TIM markers. (D) Same as (C) but for *APOE*, a DAM marker, *Skap1*, a T cell marker, *Ngp*, a neutrophil marker, and *Ebf1*, a B cell marker. (E) Footprinting of Tn5 insertion frequency around CEBPD and NFkB2 motifs. (F) Perturbation simulation plots ablating *Sox5*. Expression of the transcription factor was set to 0 and the gene regulatory networks were re-initialized to generate new expression profiles for each cell. Cells are projected in a PCA space defined by the gene regulatory net. Arrow shade indicates the magnitude of the transition flow. (G) Same as (F) but for *Klf4*. (H) Boxplot of highest-scoring ligand:receptor complexes across all microglial clusters.

Tabula Muris Senis, 2020

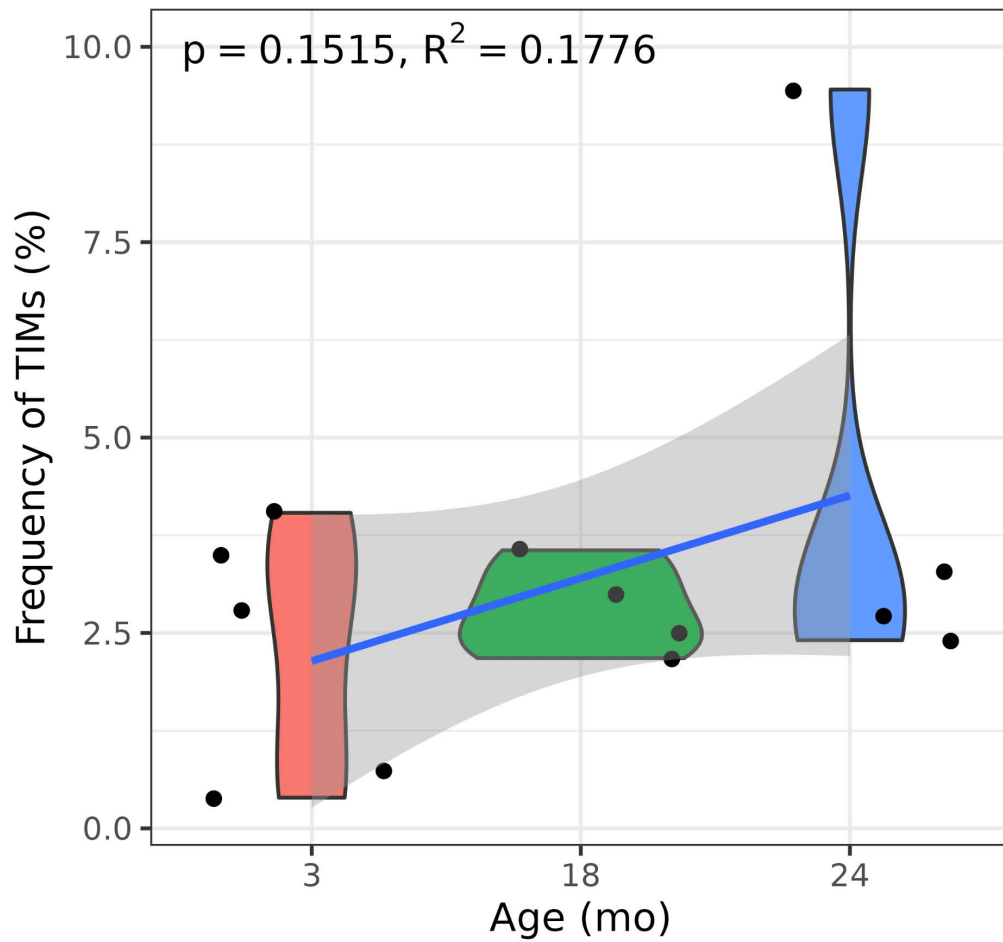
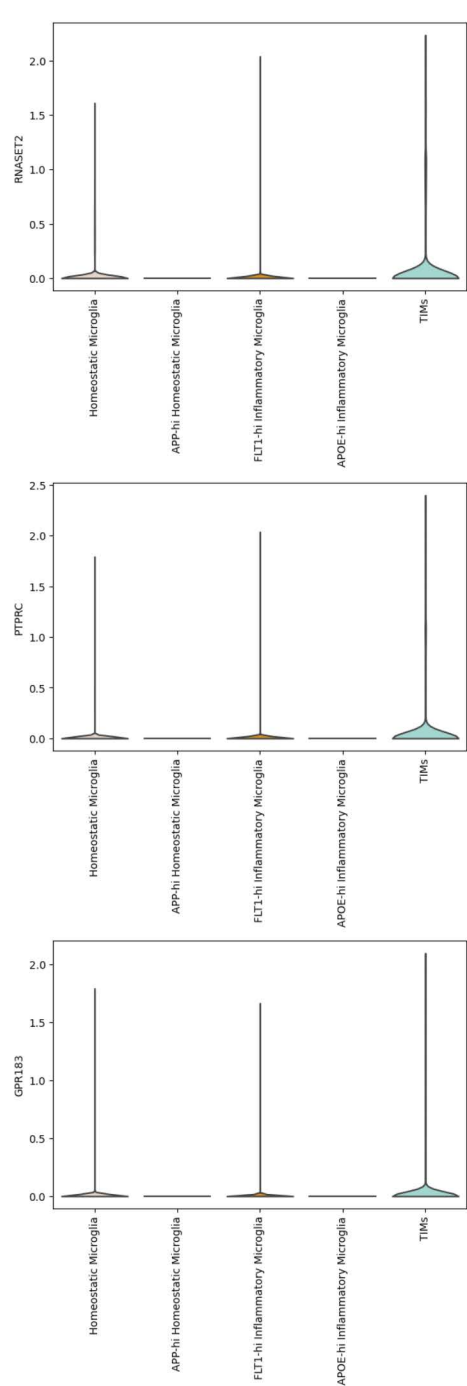
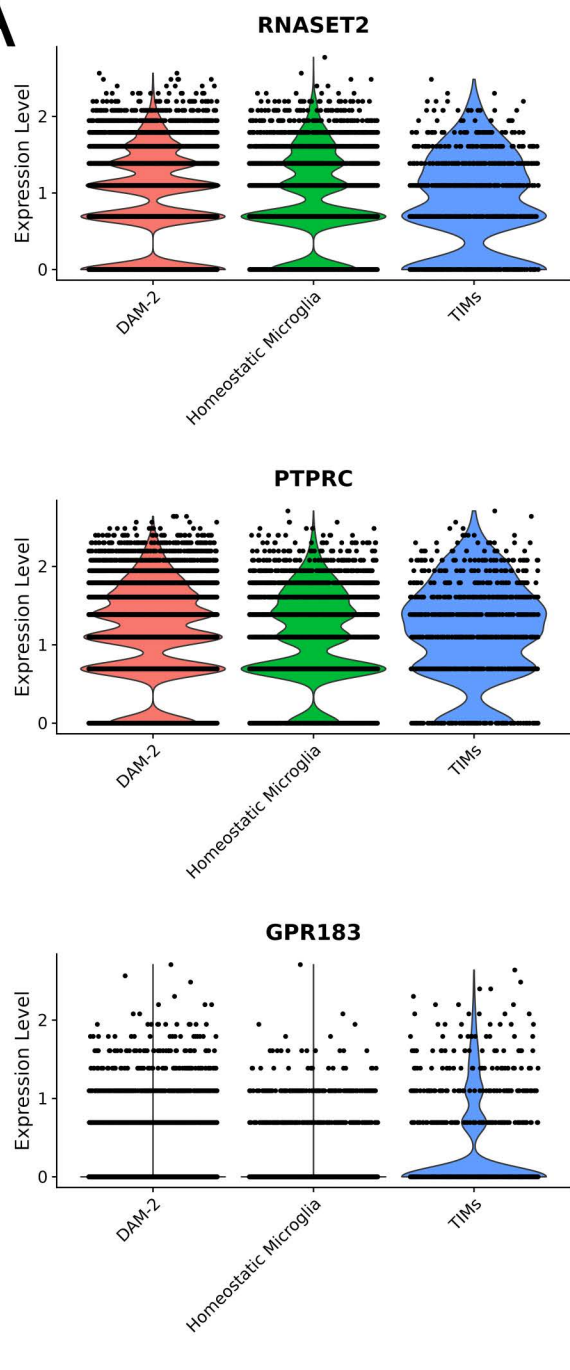
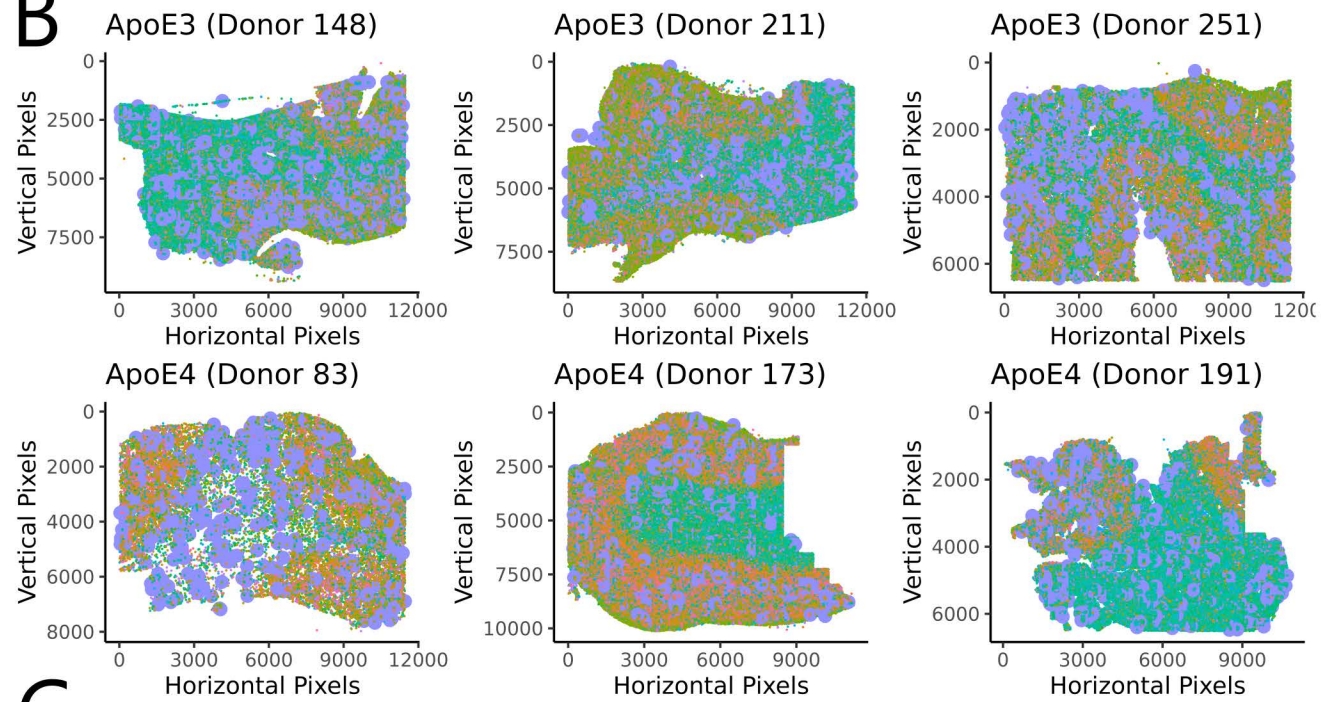


Figure S4, Related to Figure 4: Tabula Muris Senis reanalysis. Violin plot of the frequency of TIMs across each sample in the Tabula Muris Senis, a publicly available single-cell dataset of murine tissues across age. Data is overlaid with a linear regression.

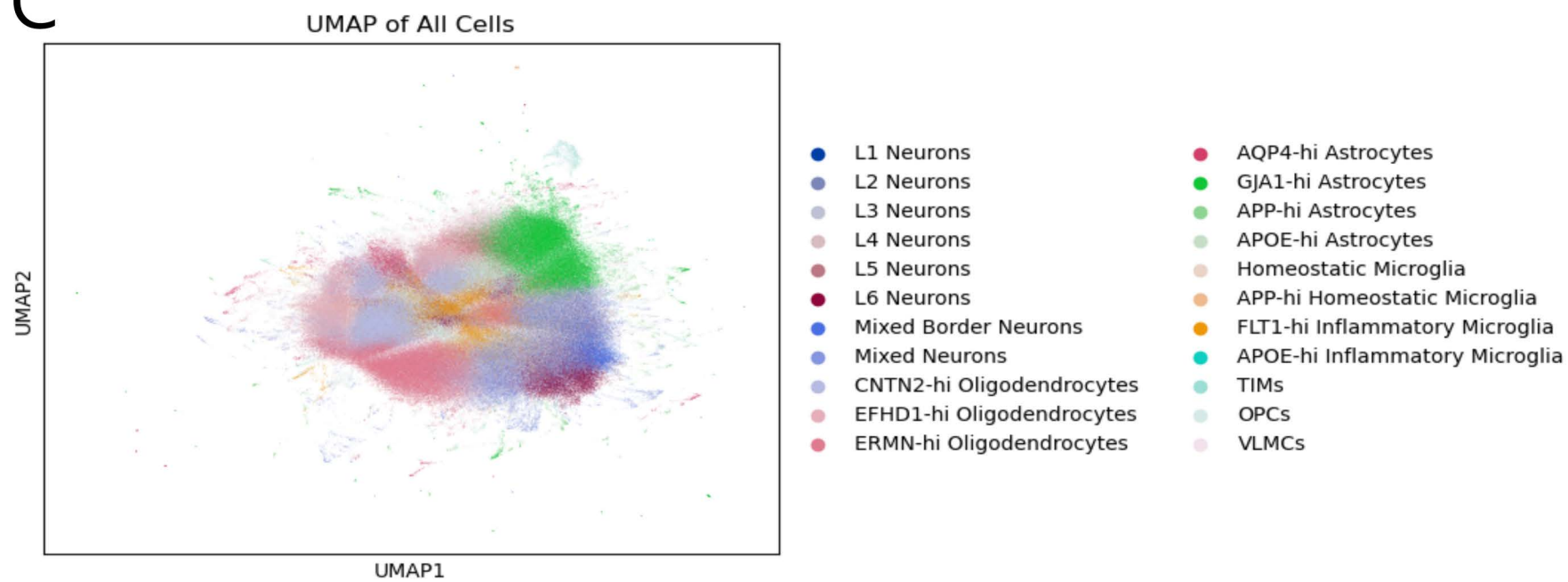
A



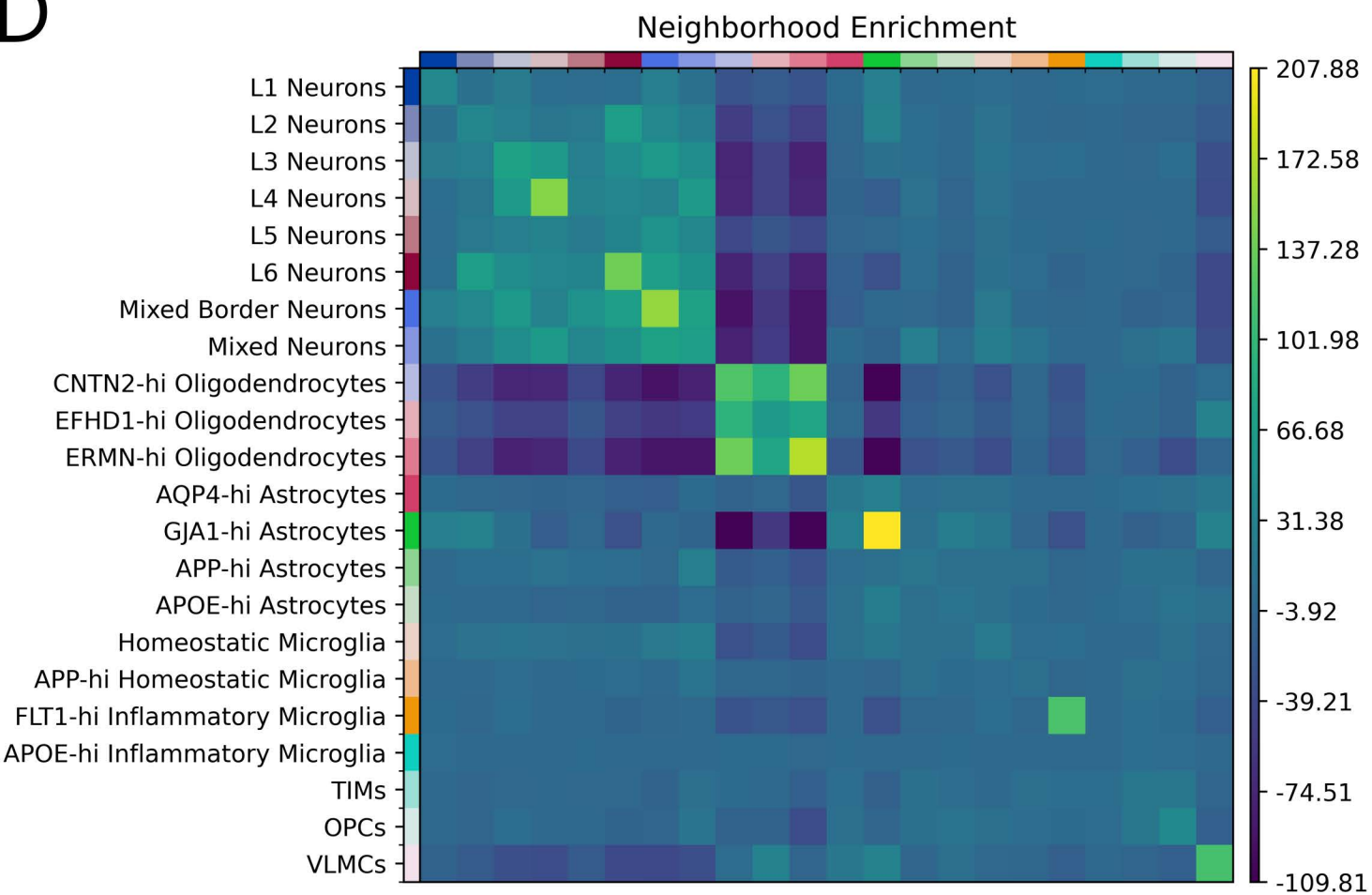
B



C



D



E

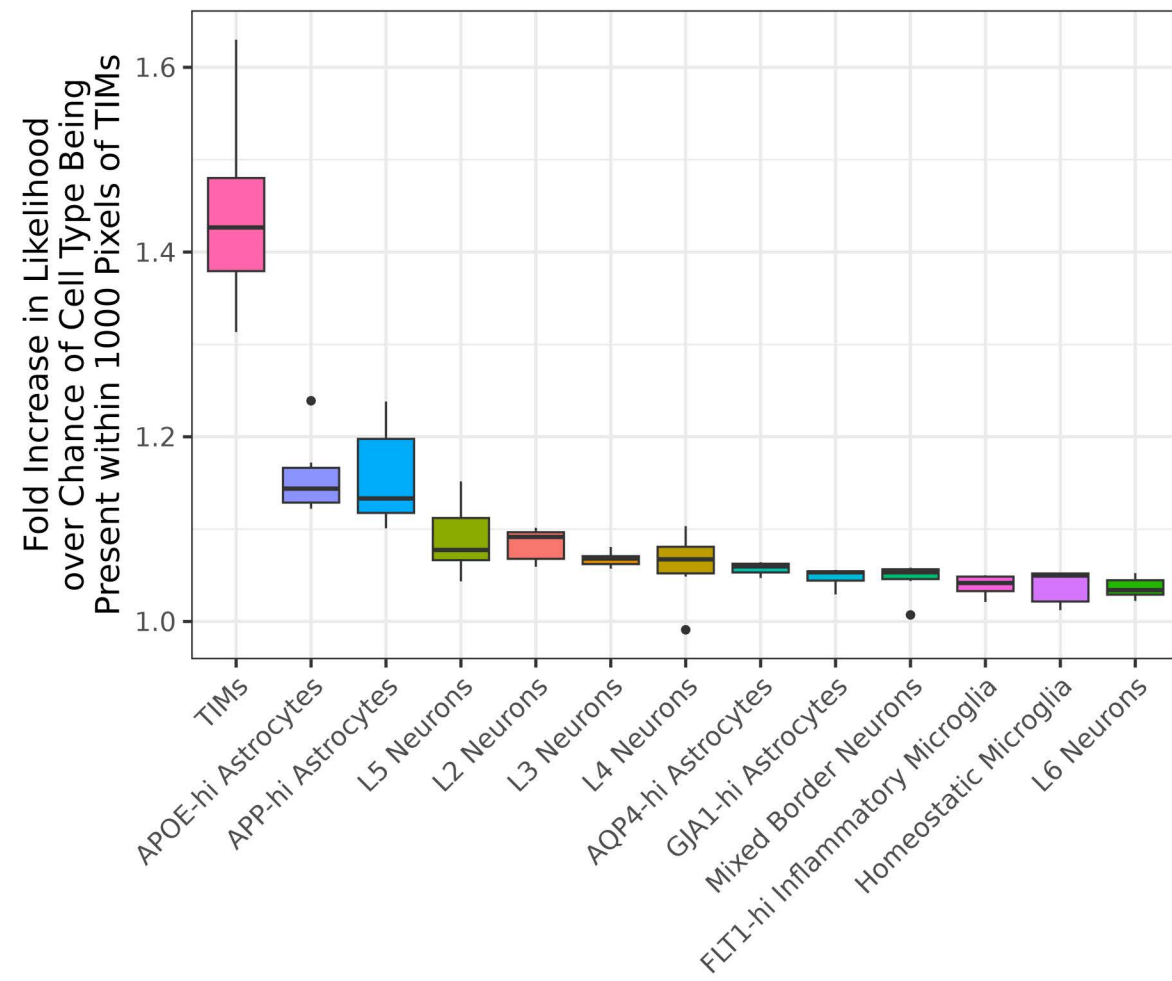
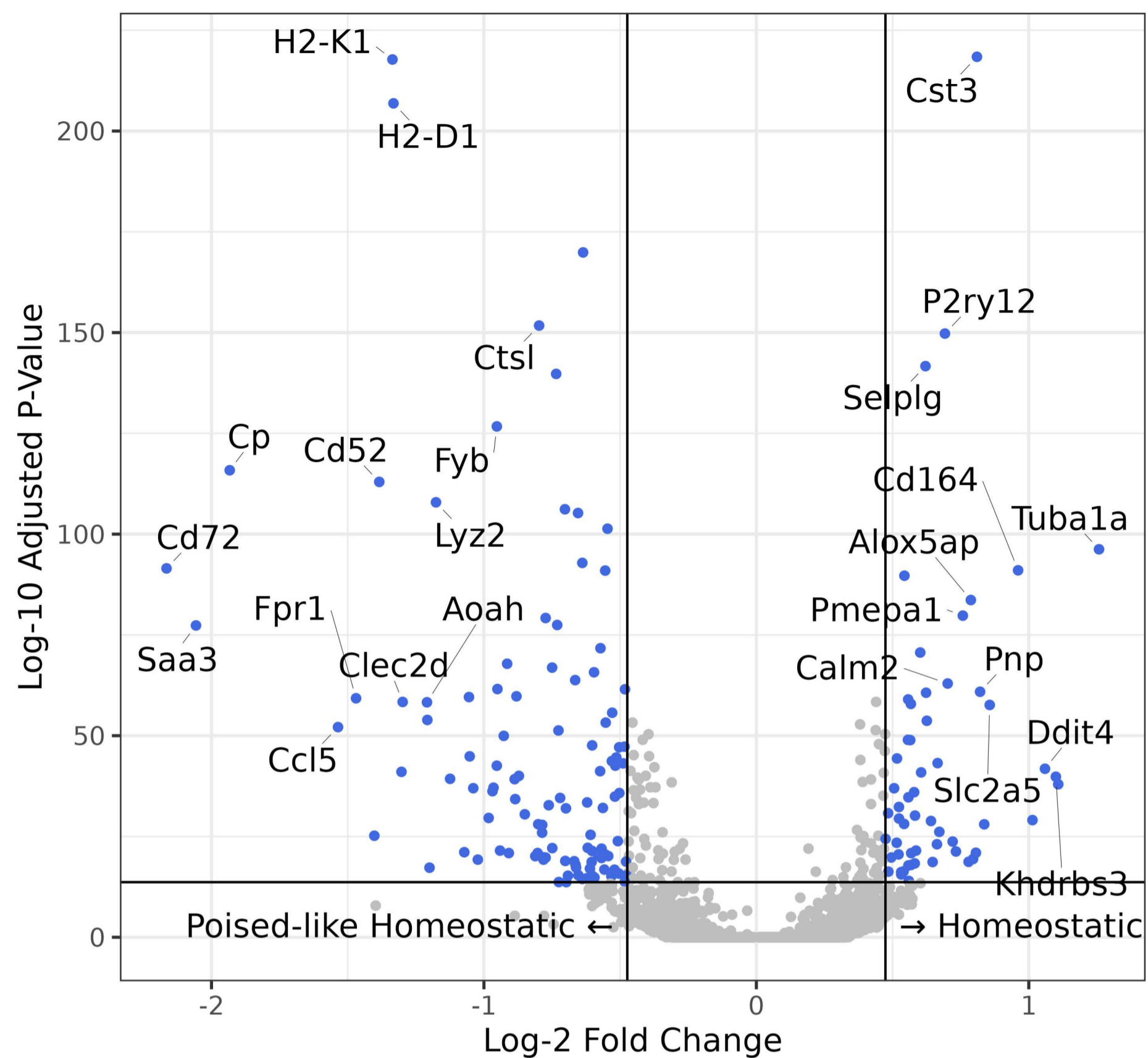
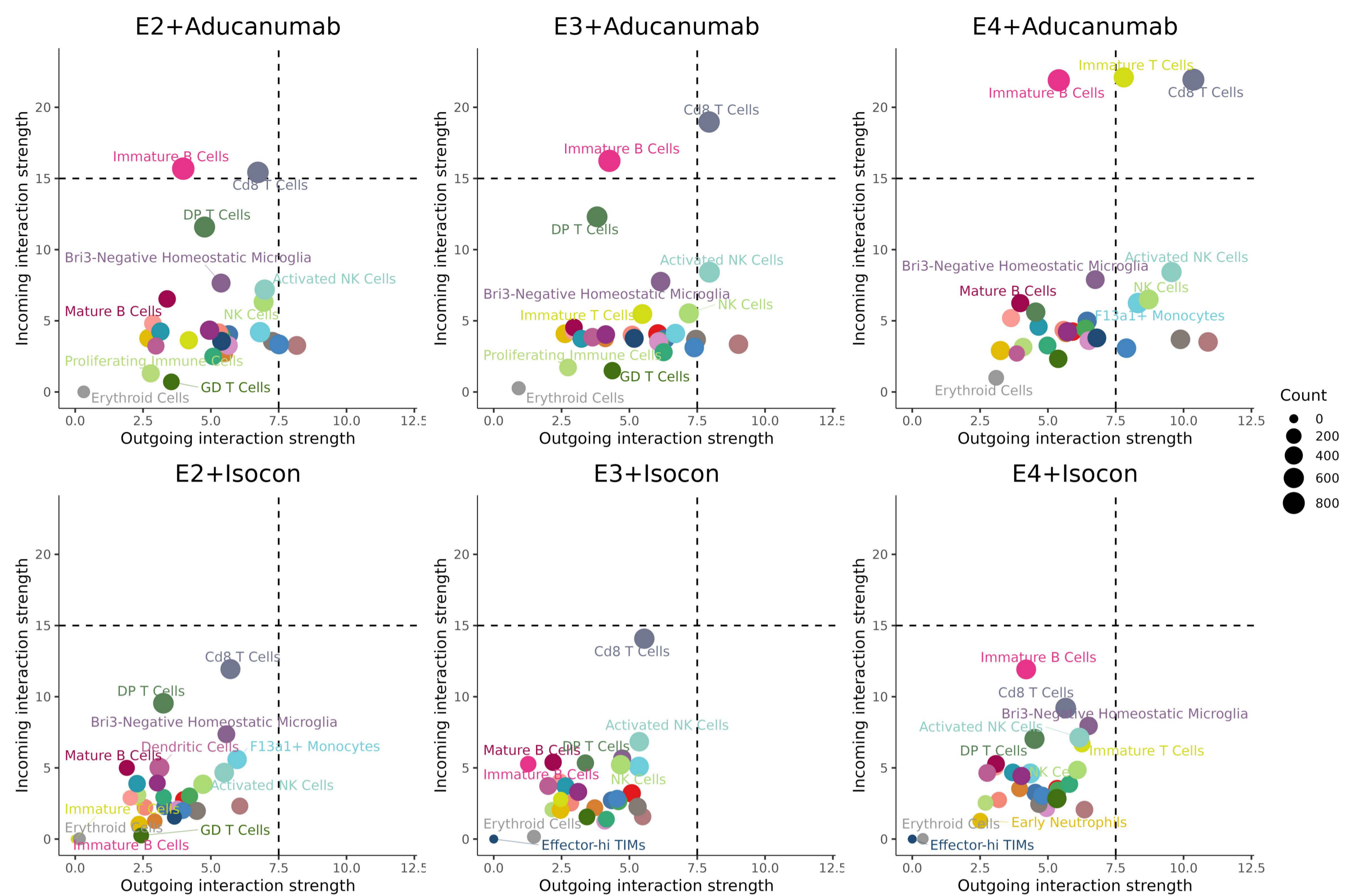


Figure S5, Related to Figure 5: Further analysis of the Xenium dataset. (A) Violin plots of three representative genes used to annotate TIMs. At left is their expression in the DLPFC-2 dataset, while at right is their expression in the Xenium data. (B) Spatial scatter plots of all six tissue sections. (C) UMAP of all 494,376 cells across all six sections, colored by final annotation. (D) Cell-cell neighborhood adjacency matrix showing the relative frequency at which cells are found adjacent to other cells *in situ* across all samples. (E) Boxplots of the increased frequency of finding a given cell within a 1000 pixel-radius circle centered around a TIM compared to a null distribution based on cell frequencies.

A



B



C

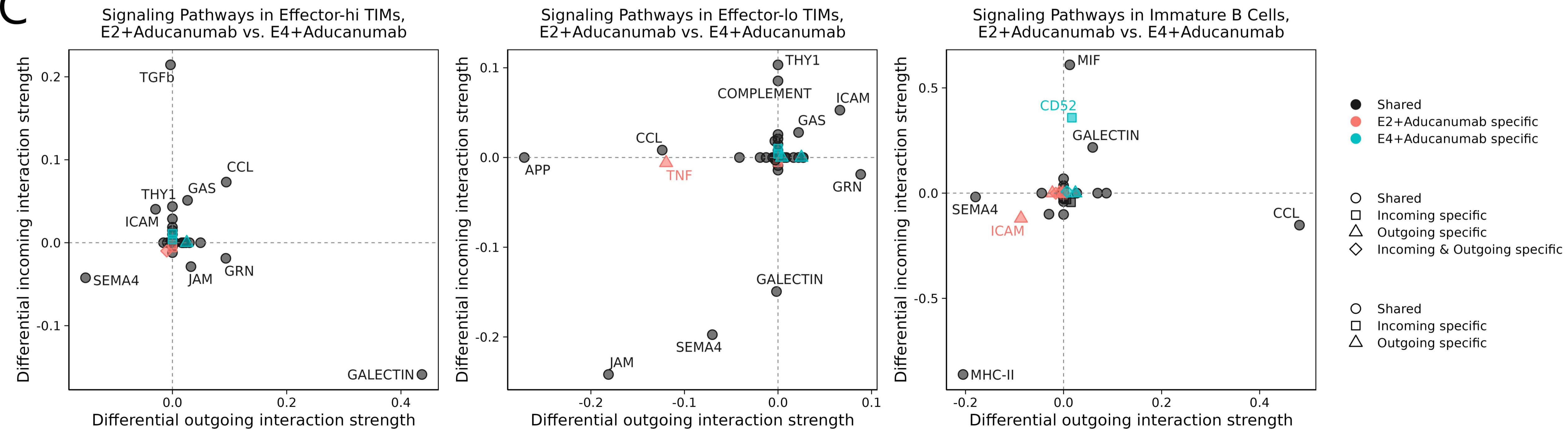


Figure S6, Related to Figure 7: Further analysis of the aducanumab dataset. (A) Violin plot of differentially expressed genes between homeostatic microglia and poised-like homeostatic microglia. (B) Dotplot of clusters in each library within the aducanumab dataset plotting incoming signaling against outgoing signaling as estimated by CellChat. (C) Dotplot of differentially enriched signaling pathways in effector-hi TIMs, effector-lo TIMs, and immature B cells between AD**APOE2* and AD**APOE4* aducanumab-treated animals by both incoming and outgoing signal strength. Pathways are color- and shape-coded by directionality and sample specificity. Positive numbers indicate a greater strength in AD**APOE4*.